

INTERNATIONAL SOCIETY FOR SOIL MECHANICS AND GEOTECHNICAL ENGINEERING



This paper was downloaded from the Online Library of the International Society for Soil Mechanics and Geotechnical Engineering (ISSMGE). The library is available here:

<https://www.issmge.org/publications/online-library>

This is an open-access database that archives thousands of papers published under the Auspices of the ISSMGE and maintained by the Innovation and Development Committee of ISSMGE.

The paper was published in the proceedings of the 10th International Conference on Physical Modelling in Geotechnics and was edited by Moonkyung Chung, Sung-Ryul Kim, Nam-Ryong Kim, Tae-Hyuk Kwon, Heon-Joon Park, Seong-Bae Jo and Jae-Hyun Kim. The conference was held in Daejeon, South Korea from September 19th to September 23rd 2022.

Physical modelling of the voluminous spill and migration of LNAPL contaminants in unsaturated soil

A. Behdad & M. Moradi

School of Civil Engineering, College of Engineering, University of Tehran, Tehran, Iran

ABSTRACT: Non-aqueous phase liquid (NAPL) is enumerated among the most critical contamination sources of soil and the water resources underlying it. In order to store these substances, sizeable underground storage tanks (USTs) are used. Consequently, the probability of NAPL spilling into the soil environment is relatively high as a result of leakage from such storage. In the current study, an N_g test was utilized for the physical modeling of this phenomenon; Moreover, the LNAPL was considered as the contaminant phase. A proto-type volume of 76.8 m^3 LNAPL was released into the unsaturated sandy soil under the gravitational field equal to 40 g . For determining the migration pattern and the LNAPL concentration, the LRV method from the consecutive images was used. Three distinct phases were observed in the LNAPL migration. Through the initial hours following the spill, vertical spread dominated the migration pattern. The downward movement continued until reaching the groundwater table, followed by the lateral spread phase of the LNAPL plume. Noticeable LNAPL infiltration into the saturated zone, particularly below the groundwater, caused vast groundwater contamination. The LNAPL phase eventually accumulated in a pool-shaped due to its lighter density than water.

Keywords: LNAPL Contaminants Transport, Unsaturated Soil, Physical Modeling, Sandy Soil.

1 INTRODUCTION

Placement of various contaminating resources near the rural and urban environments potentially threatens the soil environment, along with the aquifers. Pipelines, gas stations, refineries, and pesticides are among some examples of such resources. Geo-environmental hazards associated with such resources are growing concerns in different societies.

LNAPL contaminants are a matter of concern due to their quick dispersion in the soil environment and their negative impact on groundwater resources. For the sake of storage of these substances, sizeable underground storage tanks (USTs) are mainly used. Consequently, the LNAPL spill due to the leakage or explosion of these USTs seems quite probable, causing vast and severe subsurface contamination.

The investigation of LNAPL migration in the subsurface generally can be carried out with three various approaches. Numerical exercises are not able to provide robust predictions as the result of inherently sophisticated and known input variables. Furthermore, field investigations have been proven to be expensive as well as time-consuming. On the other hand, physical modelling approaches, particularly N_g modelling, privilege multiple advantages such as reconstituting the gravitational tensions, along with exponentially accelerating the multiphase transport in the soil.

Table 1 presents the scaling law for the N_g modelling of multiphase flow in soils.

Table 1. Scaling law for N_g modelling of multiphase flow in soils.

Parameter	Scaling Factor
Gravity	N
Length	$1/N$
Mass	$1/N^3$
Density	1
Viscosity	1
Interfacial Tension	1
Intrinsic Permeability	1
Hydraulic Conductivity	N
Time	$1/N^2$

These scaling laws were first introduced and well documented by (Arulanandan et al., 1988).

A number of efforts have been performed since then.

Two-dimensional visualization of the LNAPL migration was provided using the transparent front by (Esposito et al., 1999). Multispectral image processing was utilized in several studies to capture a continuous migration pattern throughout the timeframe, as well as the saturation content of the LNAPL phase in soil. (Kechavarzi et al., 2005; Kechavarzi et al., 2008; Zhao et al., 2015). Through the image processing method, the optical density of each pixel is correlated to the saturation of the LNAPL phase based on the color contrast.

The long-term fate and distribution of an LNAPL called "BTEX" were studied in the work of (Lo and Hu, 2004). The difference between LNAPL migration

patterns in over-consolidated and normally consolidated soils was demonstrated by (Pasha et al., 2013).

Many attempts have focused on the simulation of various LNAPL remediation methods in soil, including the soil vapor extraction (SVE) method (Hu et al., 2006), in-situ flushing method (Pasha et al., 2011), impermeable sheets, and soil-cement barriers (Kererat et al., 2013). The optimum length of soil-cement barriers for full confinement of LNAPL plume was recommended by (Behdad et al., 2021) in two different conditions.

Despite numerous potential capabilities of the N_g modelling in the simulation of multiphase flow, also the contaminants transport, the number of such studies is limited; Therefore, extensive insight into this ground has not been reached yet. Considering the results of previous works, the migration pattern and the LNAPL plume shape highly depend on the multiple field variables, such as the soil fabric and mineralogy, soil density and tension history, the amount of released LNAPL, the depth of vadose zone, the level of groundwater, interfacial tensions, soil suction status, and unsaturated parameters. Hence, laboratory simulation of multiphase flow under different circumstances seems essential regarding the serious limitations of numerical models.

The current study sheds light on the voluminous spill of LNAPL from a UST. Aside from the specific field condition of this study, the LRV image processing method was utilized to determine the extent of the contaminated area, as well as the localized LNAPL concentration through various timeframes, while previous studies mainly interpreted the N_g tests results using numerical codes.

2 MATERIALS, CONFIGURATION, AND METHOD

2.1 Test setup and constant variables

The N_g test was conducted at 40 g (40 times bigger than the earth's gravitational field.) using the geotechnical centrifuge apparatus in the physical modelling laboratory of the University of Tehran. Figure 1 demonstrates the side view of the geotechnical centrifuge at the University of Tehran.

The test's setup was composed of seven components, including the geotechnical centrifuge, strongbox, LNAPL container, LNAPL spill system, sensors, transferring instrument, imaging system, and lighting system. Figure 2 indicates the final setup of the N_g test after installation.



Fig. 1. Geotechnical centrifuge at the University of Tehran.



Fig. 2. Final setup of N_g test after installation.

During the test, 1.2 lit LNAPL (equal to 76.8 m^3 in prototype) was released into the soil. Filtered petroleum was selected as the LNAPL due to its high color contrast and low volatility.

2.2 Test's configuration and materials

Firuzkuh sand with different types of No. 181, No 161 and, a combination of No. 141 and No. 131, each representing a specific grain size, were used in different layers of the sample. The geotechnical properties of these sands have been presented in Table 2.

Table 2. Geotechnical properties of Firuzkuh sands.

Sand Type	e_{\min}	e_{\max}	D_{50} (mm)	Hydraulic Conductivity
F. Sand No. 131	0.629	0.924	0.5	9×10^{-2}
F. Sand No. 141	0.675	0.917	0.43	
F. Sand No. 161	0.658	0.91	0.27	4.5×10^{-2}
F. Sand No. 181	0.64	0.902	0.23	3.5×10^{-2}

Figure 3 demonstrates the schematic view of the model's configuration and the layers' fabric and density.

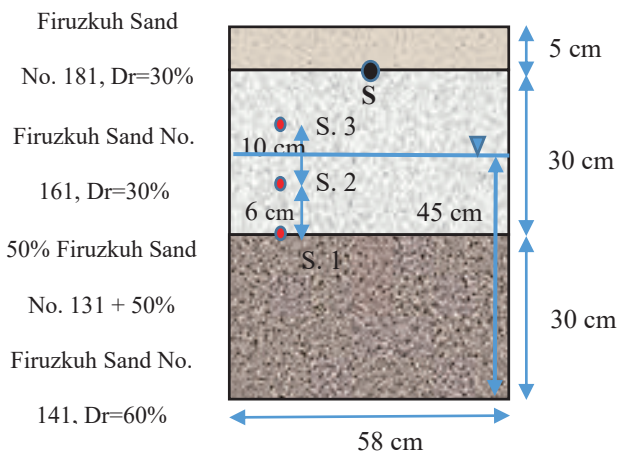


Fig. 3. Schematic view of the model's configuration.

2.3 Test procedure

The soil layers were poured and compacted using the moist tamping method. Following the strongbox and the soil sample carriage to the geotechnical centrifuge basket, water was set on the desired level using the fluid valves in the side fronts of the strongbox. During the test, the level of groundwater was recorded by the pore pressure sensors. Then the groundwater level was back-calculated.

Once the geotechnical centrifuge reached the acceleration of 40 g, the LNAPL was released from the container using a button outside the test chamber. During the spin, consecutive images were taken from the transparent front of the strongbox. Then, these images were analyzed to calculate the localized saturation of the LNAPL phase, the LNAPL plume shape, migration pattern, and the total area of the contaminated zone in different timeframes. For the image processing analysis, MATLAB software was utilized. In the LRV image processing method used in the current study, the optical density of each pixel in the image was correlated to the saturation content of the location equal to that pixel in the image. The correlation was achieved via a calibration under the same optical condition.

In order to evaluate the accuracy of the image processing method, three validation approaches were implemented following the test. Firstly, the uniformity of the plume was visually checked by digging the sectional trenches at different depths. Secondly, the mass balance analysis was performed and, the results were compared to the total volume of the released LNAPL. Finally, Localized sampling was done, and the LNAPL saturation was compared to that of the image processing. Overall, image processing accuracy in this investigation was calculated at approximately over 88 %.

3 RESULTS

Through the first phase of migration, occurring during the initial 24 hours subsequent to the spill commencement, the LNAPL movement was downward due to the dominance of gravitational forces. Similarly, the LNAPL plume was expanded in the vertical direction throughout the unsaturated zone. This vertical expansion continued until the plume's front reached the groundwater table. Consequently, it can be said that the LNAPL phase passed the continuous capillary, as well as capillary fringe, in the unsaturated profile during the initial 24 hours. Figure 4 presents the LNAPL plume in 24 hours (in prototype) following the spill.

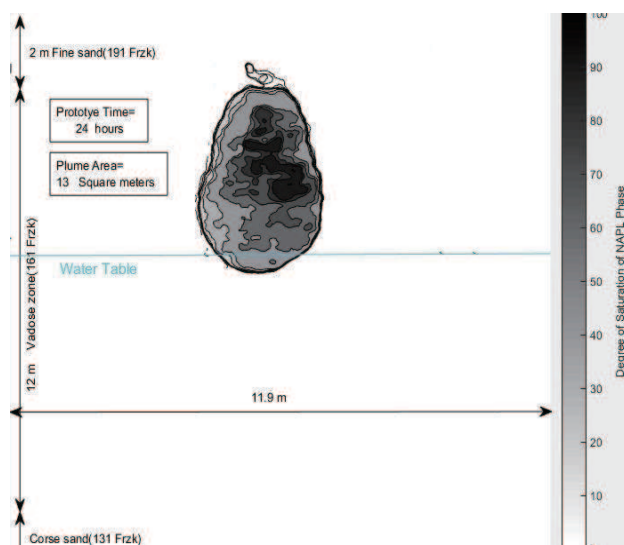


Fig. 4. LNAPL saturation and plume shape 24 hours following the spill.

In the second phase of the migration, the plume predominantly spread horizontally along with the groundwater table. The lateral expansion of the plume happened after the infiltration of the plume's front into the groundwater, which caused the dissipation of the hydraulic head of the LNAPL phase. In the second phase, the LNAPL phase was moved mainly under the influence of the interfacial and capillary forces.

The lateral spread of the plume plays a vital role in contaminating the groundwater resources and increase in the area of the contaminated zone. Figure 5 depicts the progress of the LNAPL plume on day 7 (in the prototype) following the spill.

The third and final phase of the migration is characterized by a stable condition of the LNAPL plume. In this phase succeeding the dissipation of the hydraulic head of the LNAPL phase, the LNAPL phase was expelled by the aqueous phase from the soil's pores.

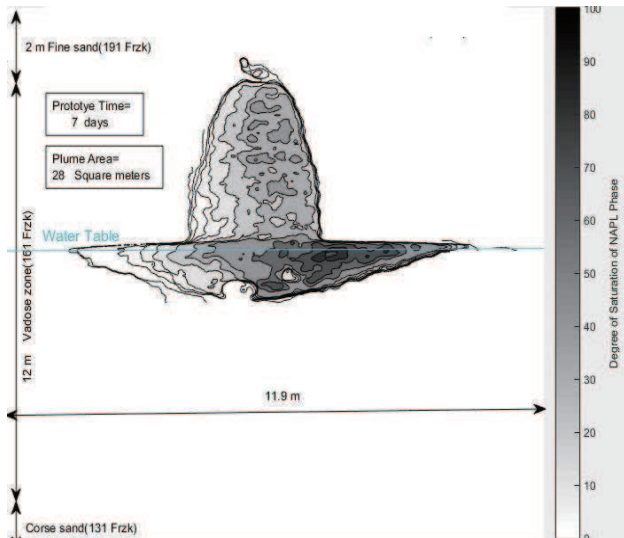


Fig. 5. LNAPL saturation and plume shape 7 days following the spill.

Therefore, the plume reached an immobile state where the LNAPL phase was accumulated with the highest concentration in the vicinity of the groundwater with a localized saturation of over 90%. This accumulation formed a pool-shaped LNAPL plume due to its lower density than that of water.

Through the final phase, taking place between days 15 and 20 under the condition of the current investigation, the maximum lateral expansion of the plume was observed, equal to 10.4 m on the prototype scale. Furthermore, the maximum vertical expansion of the plume in this time frame was recorded equal to 6.7 m in the prototype.

Figure 6 demonstrates the final fate of the LNAPL plume.

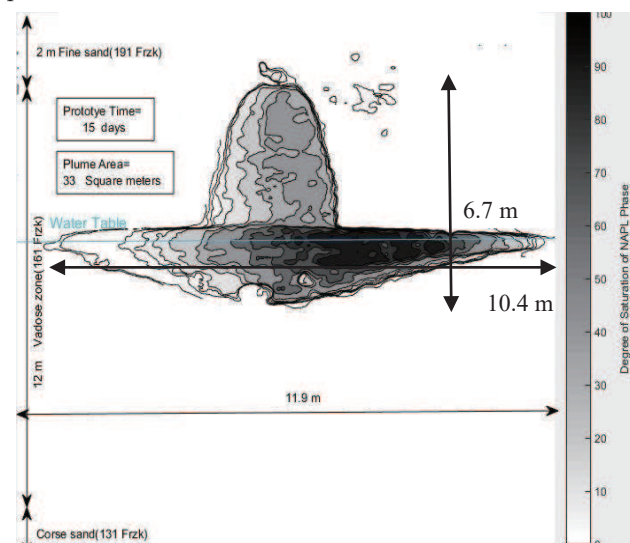


Fig. 6. LNAPL saturation and plume shape 15 days following the spill.

4 CONCLUSIONS

The following conclusions can be drawn from the current study:

1- The migration of LNAPL occurred in three distinct phases: vertical expansion, lateral expansion and, pooling accumulation, complying with the results from the previous studies.

2- The later expansion ought to be considered critical regarding the extent of contaminated zone both in the unsaturated soil and the groundwater.

3- The depression of groundwater as a result of LNAPL infiltration was observed. Moreover, the highest concentration of LNAPL was seen in the vicinity of the groundwater table.

REFERENCES

- Arulanandan, K., Thompson, P.Y., Kutter, B.L., Meegoda, N.J., Muraleetharan, K.K. and Yogachandran, C. 1988. Centrifuge modeling of transport processes for pollutants in soils. *Journal of Geotechnical Engineering* 114(2): pp.185-205.
- Behdad, A., Moradi, M. and Afshari Aghajari, A. 2021. The Effect of Soil-Cement Barriers in Containing the LNAPL Contaminants Transport in Unsaturated Soil: A Physical Modeling. *Soil and Sediment Contamination: An International Journal*: pp.1-23.
- Esposito, G., Allersma, H.G.B. and Selvadurai, A.P.S. 1999. Centrifuge modeling of LNAPL transport in partially saturated sand. *The Journal of geotechnical and geoenvironmental engineering* 125(12): pp.1066-1071.
- Hu, L.M., Lo, I.M. and Meegoda, J.N. 2006. Centrifuge testing of LNAPL migration and soil vapor extraction for soil remediation. *Practice Periodical of Hazardous, Toxic, and Radioactive Waste Management*. 10(1): pp.33-40.
- Kechavarzi, C., Soga, K. and Illangasekare, T.H. 2005. Two-dimensional laboratory simulation of LNAPL infiltration and redistribution in the vadose zone. *Journal of contaminant hydrology*. 76(3-4): pp.211-233.
- Kechavarzi, C., Soga, K., Illangasekare, T. and Nikolopoulos, P. 2008. Laboratory study of immiscible contaminant flow in unsaturated layered sands. *Vadose Zone Journal*. 7(1): pp.1-9.
- Kererat, C., Sasanakul, I. and Sorulump, S. 2013. Centrifuge modeling of LNAPL infiltration in granular soil with containment. *Journal of geotechnical and geoenvironmental engineering*. 139(6): pp.892-902.
- Lo, I.M. and Hu, L.M. 2004. Long-term migration of light nonaqueous-phase liquids in two unsaturated soils: clayey silt and fine sand. *Practice Periodical of Hazardous, Toxic, and Radioactive Waste Management*. 8(4): pp.228-237.
- Pasha, A.Y., Aflaki, E., Hu, L. and Meegoda, J.N. 2013. Effect of soil fabric on transport of a LNAPL through unsaturated fine-grained soils: a centrifugal model study. *Soil and Sediment Contamination: An International Journal*. 22(2): pp.223-240.
- Pasha, A.Y., Hu, L., Meegoda, J.N., Aflaki, E. and Du, J., 2011. Centrifuge modeling of in situ surfactant enhanced flushing of diesel contaminated soil. *Geotechnical Testing Journal*. 34(6): pp.623-633.
- Zhao, Y., Sun, J., Sun, C., Cui, J. and Zhou, R. 2015. Improved light-transmission method for the study of LNAPL migration and distribution rule. *Water Science and Technology*. 71(10): pp.1576-1585.